ARTICLE OPEN

Check for updates

Intravenous psilocybin induces dose-dependent changes in functional network organization in rat cortex

Brian H. Silverstein[1,2,8], Nicholas Kolbman[1,2,3,8], Amanda Nelson[1], Tiecheng Liu[1], Peter Guzzo[4], Jim Gilligan[4], UnCheol Lee[1,2,5], George A. Mashour[1,2,3,5,6], Giancarlo Vanini[1,2,5,6,9] and Dinesh Pal[1,2,5,6,7,9]✉

Psilocybin produces an altered state of consciousness in humans and is associated with complex spatiotemporal changes in cortical networks. Given the emphasis on rodent models for mechanistic studies, there is a need for characterization of the effect of psilocybin on cortex-wide network dynamics. Previous electroencephalographic studies of psychedelics in rodents have primarily used sparse electrode arrays with limited spatial resolution, precluding network level analysis, and have been restricted to lower gamma frequencies. Therefore, in this study, we used electroencephalographic recordings from 27 sites/electrodes across rat cortex ($n = 6$ male, 6 female) to characterize the effect of psilocybin (0.1, 1, and 10 mg/kg delivered over an hour) on brain network organization as inferred through changes in node degree (an index of network density) and connection strength (via weighted phase-lag index). The removal of aperiodic component from the electroencephalogram localized the primary oscillatory changes to theta (4–10 Hz), medium gamma (70–110 Hz), and high gamma (110–150 Hz) bands, which were used for the network analysis. Additionally, we determined the concurrent changes in theta-gamma phase-amplitude coupling. We report that psilocybin, in a dose-dependent manner, 1) disrupted theta-gamma coupling [$p < 0.05$], 2) increased frontal high gamma connectivity [$p < 0.05$] and posterior theta connectivity [$p \leq 0.049$], and 3) increased frontal high gamma [$p < 0.05$] and posterior theta [$p \leq 0.046$] network density. The behavioral activity and the medium gamma frontoparietal connectivity showed an inverted-U relationship with psilocybin dose. Our results suggest that high-frequency network organization, decoupled from local theta-phase, may be an important signature of psilocybin-induced non-ordinary state of consciousness.

Translational Psychiatry (2025)15:93 ; https://doi.org/10.1038/s41398-025-03308-4

INTRODUCTION

Psilocybin is a serotonergic psychedelic that is being explored in clinical trials to treat psychiatric disorders [1–6]. In humans, psilocybin produces an altered state of consciousness, associated with complex changes in brain network activity including increased posterior connectivity and decreased frontal connectivity [7], increased spatiotemporal complexity [8–10], decreased network segregation [11], and decreased spectral power and connectivity in low (<40 Hz) frequencies [12–14]. Functional connectivity changes have also been shown to correlate with psychedelic-induced subjective experiences, suggesting network dynamics may be an important component of the mechanisms underpinning the action of psychedelic drugs, including psilocybin [12, 15–17]. Recent electrophysiological studies in rodents suggest that the emergence of high gamma (>110 Hz) amplitude and connectivity, observed during administration of lysergic acid diethylamide (LSD), ketamine, and phencyclidine, may be an important common marker of psychedelics [18–20]. However, this high gamma emergence phenomenon has not been investigated during psilocybin administration, and previous animal studies using psilocin or intracranial recordings after systemic delivery of psilocybin lacked the spatial resolution to allow corticocortical network analysis [21–23]. Relatedly, gamma amplitude is known to be modulated according to the phase of theta band (4–10 Hz) oscillations, and it has been demonstrated that the relationship between these two frequency bands changes with cognitive demands and state of arousal [24–27]. If local and interregional gamma-range dynamics are altered by psychedelic administration, disruption of theta-gamma coupling is likely a correlated phenomenon. However, psilocybin-induced theta-gamma decoupling has not been systematically demonstrated in rodents with co-occurring network-level changes.

Therefore, in this study, we used cortex-wide high-density (27 electrodes) electroencephalographic recordings to characterize the effect of psilocybin (0.1, 1, and 10 mg/kg) delivered intravenously over an hour, in Sprague Dawley rats. We first performed spectral decomposition of the electroencephalogram (EEG) data to identify the primary oscillatory components that were affected by psilocybin. These analyses showed that psilocybin altered three oscillatory components in the theta (4–10 Hz), medium gamma (70–110 Hz), and high gamma (110–150 Hz) bands, which were used to further analyze the

[1]Department of Anesthesiology, University of Michigan, Ann Arbor, MI, USA. [2]Center for Consciousness Science, University of Michigan, Ann Arbor, MI, USA. [3]Department of Pharmacology, University of Michigan, Ann Arbor, MI, USA. [4]Tryp Therapeutics, Kelowna, BC, Canada. [5]Michigan Psychedelic Center, University of Michigan, Ann Arbor, MI, USA. [6]Neuroscience Graduate Program, University of Michigan, Ann Arbor, MI, USA. [7]Department of Molecular & Integrative Physiology, University of Michigan, Ann Arbor, MI, USA. [8]These authors contributed equally: Brian H. Silverstein, Nicholas Kolbman. [9]These authors jointly supervised this work: Giancarlo Vanini, Dinesh Pal. ✉email: dineshp@umich.edu

Received: 12 March 2024 Revised: 23 January 2025 Accepted: 11 March 2025
Published online: 25 March 2025

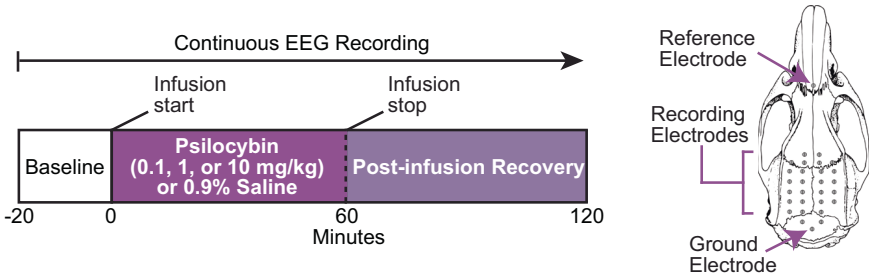

Fig. 1 Schematics showing the experimental design and timeline. Each rat ($n = 12$, 6 male, 6 female) received 0.9% saline and three doses of psilocybin (0.1, 1, and 10 mg/kg) as a continuous infusion over the course of an hour. Each infusion session was separated by 5–7 days and was conducted in a random order. On the right-side of the experimental timeline, an image of the rat cranium indicating the EEG, ground, and reference electrode locations is shown.

changes in phase-amplitude coupling and network organization. We report that psilocybin disrupted theta-gamma coupling and induced multiscale reorganization of cortical connectivity, as shown by simultaneous increase in frontal high gamma connectivity and posterior theta connectivity, and a decrease in posterior medium gamma network connectivity. Our results also show increased posterior theta and frontal high gamma network density, which is a measure of the number of functional connections at any given electrode. These findings suggest that high-frequency network reorganization, decoupled from local theta-phase, may be an important signature of the non-ordinary state produced by psilocybin.

MATERIALS AND METHODS

Adult Sprague Dawley rats ($n = 12$, 6 male, 6 female, weight 300–350 g, Charles River Laboratories Inc., Wilmington, MA) maintained on 12 h: 12 h light: dark cycle (lights ON at 8:00 am) and with *ad libitum* food and water, were used for all experiments. The experiments were approved by the Institutional Animal Care and Use Committee at the University of Michigan, Ann Arbor, and were conducted in compliance with the Guide for the Care and Use of Laboratory Animals (Ed 8, National Academies Press) and ARRIVE Guidelines [28].

Surgical procedures

Under surgical isoflurane (Piramal Enterprises, Telangana, India) anesthesia, rats were implanted with stainless steel screw electrodes (J.I. Morris Miniature Fasteners, Oxford, MA, USA; #FF000CE094) to record EEG from 27 sites across the cortex and bilateral wire electrodes (Cooner Wire Company, Chatsworth, CA, USA; # AS 636) to record electromyogram (EMG) from dorsal nuchal muscles. An in-dwelling chronic catheter (Micro-Renathane tubing, MRE-040, Braintree Scientific, MA) was positioned in the jugular vein for infusion of psilocybin (Cayman Chemical, MI; CAS 520-52-5) and 0.9% saline (Hospira, Lake Forest, IL, USA; #00409-4888-20) as vehicle control. The jugular venous catheter was flushed with 0.2 mL of heparinized (1 unit/mL, Sagent Pharmaceuticals, Schaumburg, IL) saline and locked with 0.05 mL of Taurolidine-Citrate Catheter lock solution (TCS-04, Access Technologies, Skokie, IL) every 5–7 days to maintain catheter patency. Subcutaneous buprenorphine hydrochloride (Buprenex ®, Reckitt Benckiser Pharmaceuticals Inc., Richmond, VA; 0.01 mg/kg) and carprofen (Hospira, Inc., Lake Forest, IL; 5 mg/kg) were used for pre-surgical analgesia. Post-surgical analgesia was achieved with buprenorphine hydrochloride (0.03 mg/kg) administration every 6–8 h for 48 h. All rats were allowed at least 7–10 days of post-surgical recovery, during which they were conditioned to the recording chambers and EEG acquisition system.

Experimental design

The experimental design is illustrated in Fig. 1. On the day of the experiment, rats were connected to the EEG acquisition system between 9:00 and 9:30am and allowed to habituate for a minimum of 1 h. Following habituation, baseline EEG was acquired for 20 min. Thereafter, one of the three doses of psilocybin (0.1, 1, or 10 mg/kg) was delivered (intravenous) over an hour. To control for the circadian influence and homeostatic sleep pressure, all infusions were administered between 10:30 and 11:00am. All rats received, on separate days, each of the three doses of psilocybin and vehicle control. To avoid any confound due to the order of drug-dose administration, infusion sessions - saline and three different doses of psilocybin – were conducted in a random order across rats. Of the six male rats, four received 10 mg/kg psilocybin in the first experimental session followed by 1 mg/kg psilocybin, 0.9% saline, and 0.1 mg/kg psilocybin in the subsequent sessions. The remaining two male rats received 0.1 mg/kg psilocybin in the first session followed by 1 mg/kg psilocybin, 10 mg/kg psilocybin, and 0.9% saline infusion in subsequent sessions. Of the six female rats, four received 1 mg/kg psilocybin in the first experimental session followed by 10 mg/kg psilocybin, 0.9% saline, and 0.1 mg/kg psilocybin in the subsequent sessions. The remaining two female rats received 0.1 mg/kg psilocybin in the first session followed by 0.9% saline, 1 mg/kg psilocybin, and 10 mg/kg psilocybin in the subsequent sessions. Each infusion session (0.9% saline or one of three psilocybin doses) was performed on a separate day with an interval of 5–7 days between sessions. To maintain a near-constant behavioral state of wakefulness during the infusion and post-infusion recovery period, we gently tapped on the recording chamber if slow waves appeared in the EEG.

Head twitch response and behavioral activity/locomotion

All experimental sessions were video recorded and analyzed, except for one 10 mg/kg psilocybin infusion session in a male rat. Rat activity and locomotion were captured using a 3-axis gyroscope sensor built into the EEG acquisition head-stage. The experimental conditions of the video recordings and gyroscope data files were masked to allow for blinded analysis of head-twitch response (HTR) and locomotion based on gyroscope activity. The HTR is defined as a rhythmic rotational movement of the head that occurs in rodents in response to serotonergic psychedelic-induced 5-HT2A receptor activation (See representative HTR video in the Supplemental information) [29–31]. The HTR was quantified using visual analysis of video recordings for the 5-min period prior to the start of intravenous infusion of either saline or psilocybin, and for the entirety of 60-min infusion period. HTR counts were either binned in 5-min epochs or summed for the entire 60-min infusion. The gyroscope data were binned in 10-min epochs.

Electrophysiological data acquisition

Electrophysiological signals were recorded using the Cereplex Direct recording system (Blackrock Neurotech, Salt Lake City, UT). Monopolar EEG (0.1–300 Hz, sampling rate 1 kHz) and bipolar EMG (0.1–125 Hz, sampling rate 500 Hz) were recorded continuously throughout the experiment. The EEG data acquisition head-stage was equipped with a motion sensor for which the data were bandpass filtered between 0.1–50 Hz and sampled at 500 Hz. The EEG data were manually inspected for noise and/or movement artifacts and the segments or channels with excessive noise/artifacts were excluded from further analysis. The EEG data were downsampled to 500 Hz prior to computational analysis.

Spectral analysis

Spectral characteristics of the EEG data were estimated at each channel in 2-s non-overlapping windows using a multitaper wavelet decomposition as implemented in Fieldtrip [32]. Using the FOOOF algorithm [33], we estimated the aperiodic offset and aperiodic exponent of the power spectrum and removed the 1/f component to facilitate peak frequency detection. Maximum oscillation peak for each of the theta (4–10 Hz), medium gamma (70–110 Hz), and high gamma (110–150 Hz) bands were

estimated. For statistical analysis, frequency band amplitude and peak frequency were averaged across 10-min non-overlapping windows and across channels.

Phase-amplitude coupling

Phase-amplitude coupling (PAC) was estimated for artifact-free 10-s epochs according to the method first described by Canolty [34], and expanded by Onslow [35]. PAC was computed between low frequencies (*LF;* bandpass filtered in 2 Hz steps and centered on 2–18 Hz) and high frequencies (*HF;* bandpass filtered in 5 Hz steps and centered on 27–197 Hz). Data were filtered and converted into analytic signals using a wavelet convolution (Morlet wavelet, width = 7). The instantaneous phase, θ, and amplitude, A, were extracted from each signal and combined to create a third composite signal, X, such that $X(t) = A_{HF}(t)e^{i\theta_{LF}(t)}$ where t is time. In a given time window and channel, PAC was calculated as $PAC_{raw} = |n^{-1}\sum_{t=1}^{n} X(t)|$ where n is the number of samples in a window. To ensure that values of PAC are independent of large power fluctuations or nonuniform phase distributions, we then applied permutation testing to generate normalized values of PAC in each window and channel. In each window, the amplitude time series extracted from the Morlet wavelet transformation were shuffled prior to computing a new PAC value, PAC_{shuff}. This procedure was repeated 30 times, then the mean, μ_{shuff}, and standard deviation, σ_{shuff}, were used to compute normalized PAC such that $PAC_{norm} = \frac{PAC_{raw} - \mu_{shuff}}{\sigma_{shuff}}$. Mean PAC_{norm} was computed for each 10-min epoch at each channel and at the global level. PAC_{norm} values in specific frequency band pairs, e.g. theta-medium gamma coupling, were computed by averaging PAC_{norm} values within each frequency range.

Weighted phase-lag index

Weighted phase-lag index (wPLI) is a measure of functional connectivity that estimates the consistency of the phase relationship between two signals and is robust to volume conduction [36]. To compute wPLI for a given channel pair of electrodes x and y, we first applied a FIR bandpass filter and Hilbert transform to the monopolar EEG data to extract the analytic signal of each electrode. The complex conjugate of each channel pair was next computed to estimate the cross spectrum, C_{xy}. Next, taking the imaginary component of C_{xy}, $\Im_{xy}$, wPLI was then estimated as $wPLI_{xy} = \frac{|E\{\Im_{xy}\}|}{E\{|\Im_{xy}|\}}$. To rule out spurious connectivity due to the spectral distribution, we shuffled the phases of each channel while maintaining the amplitude distribution, using an FFT-based approach [37], to compute $wPLI_{shuff}$. Analogous to the approach taken with PAC, this procedure was repeated 30 times, then the mean, μ_{shuff}, and standard deviation, σ_{shuff}, were used to compute normalized wPLI such that $wPLI_{norm} = \frac{wPLI_{raw} - \mu_{shuff}}{\sigma_{shuff}}$. The channel-pair values of $wPLI_{norm}$ were averaged to estimate global $wPLI_{norm}$. Local and global estimates of $wPLI_{norm}$ were averaged within each 10-min epoch for statistical analysis. Finally, to compute node degree, binary undirected networks were computed from $wPLI_{norm}$ by binarizing each 27×27 matrix according to a threshold of $p = 0.05$, equivalent to $wPLI_{norm} = 1.67$. Node degree is then computed by taking the sum of each row.

Statistical analyses

Statistical analyses were conducted in consultation with *the Consulting for Statistics, Computing and Analytics Research* unit at the University of Michigan (Ann Arbor, Michigan) using R (version 4.0.2). To facilitate statistical analyses, each EEG measure was averaged into 10-min non-overlapping windows. Linear mixed models were computed at the global level for spectral analysis, and behavioral – HTR and gyroscope – analysis, with rat as a random factor and dose and time as fixed factors. The sample size for each group was chosen based upon previous studies conducted in our laboratory as well as similar studies conducted by other laboratories [19–21]. We included sex as a fixed factor and did not observe any main effect of sex. However, due to a relatively small sample size for male ($n = 6$) and female ($n = 6$) cohorts, we did not do a direct statistical comparison of the effect of dose on either behavioral (HTR, movement) or EEG measures between male and female rats and have provided separate data plots for male and female rats in the Supplementary information (Supplementary Figs S1–12). For channel-level analysis, the model was repeated for each channel, post-hoc comparisons between saline and each drug condition were extracted, and associated p-values were false discovery rate (FDR)-adjusted with an alpha = 0.05. For HTR analysis, post-hoc comparisons between saline and drug conditions were extracted, the alpha threshold was set to $p < 0.05$, and associated p-values were adjusted with the Tukey method.

RESULTS

All rats were implanted with electrodes to record EEG from across the cortex and received an hour-long intravenous infusion of three different doses of psilocybin and 0.9% saline (vehicle control) on separate days in a random order with at least 5–7 days of inter-experiment interval. We focused our analysis on 90 min of EEG data comprising a 10-min pre-psilocybin infusion baseline period, 60 min spanning the intravenous administration of psilocybin (0.1, 1, and 10 mg/kg) or 0.9% saline, and 20 min immediately after the end of psilocybin or saline infusion (Fig. 1).

Dose-dependent effects of psilocybin on rat behavior

Psilocybin dose-dependently induced the HTR and resulted in a biphasic inverted U-shaped dose-effect curve over the time-course of the 60-min infusions (Fig. 2A). In the first 5 min of the infusion, 10 mg/kg psilocybin produced significantly more head-twitches as compared to that after saline, 0.1 mg/kg, and 1 mg/kg psilocybin (all $p \leq 0.0001$). Between 5–10 min, 10 mg/kg psilocybin infusion produced significantly more head-twitches as compared to saline ($p \leq 0.0001$), 0.1 mg/kg ($p \leq 0.0001$), and 1 mg/kg psilocybin ($p = 0.0028$). The 1 mg/kg psilocybin infusion produced significantly more head-twitches as compared to saline ($p = 0.0004$) and 0.1 mg/kg ($p = 0.0097$) psilocybin between 5–10 min. The 1 mg/kg psilocybin infusion also produced significantly more head-twitches as compared to that after saline ($p \leq 0.0001$), 0.1 mg/kg ($p = 0.0046$), and 10 mg/kg ($p \leq 0.0001$) psilocybin between 10–15 min of infusion. Analysis of the total number of head-twitches recorded throughout the entire 60-min infusion (Fig. 2B) revealed that as compared to saline infusion, infusion of both 1 mg/kg ($p = 0.0362$) and 10 mg/kg ($p = 0.0308$) psilocybin produced significant increases in head-twitches.

Analysis of the mean 3D angular velocity throughout the recording session showed that as compared to saline infusion, 0.1 mg/kg psilocybin had no effect on rat movement ($p > 0.05$) (Fig. 2C). The 1 mg/kg dose induced a brief period (~10 min) of increased movements after 10 min of infusion ($p = 0.0069$), after which the level of movement returned to that observed after saline infusion. The 10 mg/kg psilocybin produced a significant decrease in rat movements 30–50 min and at 70 min in the infusion period (all $p \leq 0.023$).

Psilocybin altered spectral power in theta and gamma bands and dynamically shifted dominant EEG frequencies

Comparisons of the power spectrum between each dose of psilocybin and saline control indicated that psilocybin-related changes in spectral characteristics are not broadband but localized in frequency space and shifting over time (Fig. 3A–C). In order to focus our analysis on the localized oscillatory changes, we applied the FOOOF algorithm [33] to all EEG data. The FOOOF algorithm removes the aperiodic (1/f) component from the power spectrum, enabling unbiased estimation of the peak frequency and amplitude of oscillatory components. This step is crucial to avoid confounding a change in the oscillatory peak frequency and amplitude with a change in the broadband component. Detrending the power spectrum revealed that the primary oscillatory components affected by psilocybin infusion corresponded to theta (4–10 Hz), medium gamma (70–110 Hz), and high gamma (110–150 Hz) bands (Fig. 3D).

Analysis of the peak frequency and amplitude of each component over the duration of the recording period showed that there was no statistically significant effect of 0.1 mg/kg psilocybin infusion on EEG oscillatory components ($p > 0.05$), but clear dose-dependent effects were observed during both 1 and 10 mg/kg infusions (Fig. 3E–J). Relative to saline infusion, peak frequency in the theta band (Fig. 3E) briefly increased 10 min after the start of 1 mg/kg psilocybin infusion ($p = 0.0074$), while the 10 mg/kg psilocybin produced a sustained decrease in theta peak frequency beginning after 30 min of infusion. The peak frequency

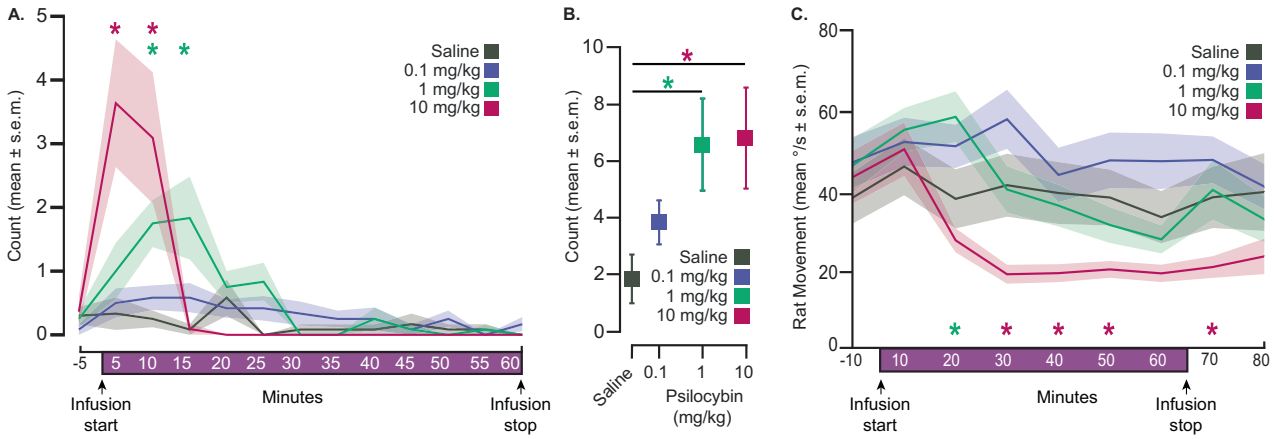

Fig. 2 Effect of intravenous psilocybin on head-twitch response and rat movement. A The head-twitch response (HTR) was quantified for the 5-min period prior to the start of intravenous infusion of psilocybin/saline, and for the entirety of the 60-min infusion period ($n = 12$, 6 male and 6 female rats for all treatment groups except for 10 mg/kg group which had 5 male rats). HTR count data are presented as group means ± standard error of the means in 5-min bins. The 10 mg/kg psilocybin infusion produced significantly more head-twitches in comparison to that observed after saline in the first 5 min of the infusion ($p \leq 0.0001$). The 10 mg/kg ($p \leq 0.0001$) and 1 mg/kg ($p = 0.0004$) psilocybin infusions produced significantly more head-twitches 5–10 min into the 60-min infusion in comparison to that observed after saline infusion. The 1 mg/kg psilocybin infusion displayed significantly more head-twitches in comparison to the saline infusion ($p \leq 0.0001$) 10–15 min into the 60-min infusion. *$p < 0.05$, Tukey post-hoc comparisons between saline and psilocybin doses. **B** Total HTR count for the entirety of each 60-min infusion was quantified and data are presented as group means ± standard error of the means. Both the 10 mg/kg ($p = 0.0308$) and 1 mg/kg ($p = 0.0362$) infusions displayed significant increases in total HTR count for the entirety of the 60-min intravenous psilocybin infusions in comparison to saline. *$p < 0.05$, Tukey post-hoc comparisons between saline and psilocybin doses. **C** 3axis gyroscope activity was averaged in 10-min bins and plotted as mean ± standard error of the mean. The 1 mg/kg dose briefly increased rat movements, whereas the 10 mg/kg dose resulted in a quiescent state with minimal movement, thereby dissociating the increased gamma power from movement. *$p < 0.05$, FDR-corrected *p*ost-hoc comparisons between saline and psilocybin doses. The exact *p* values are provided in the results section.

in medium gamma band (Fig. 3F) was significantly increased after 10 min of 1 mg/kg psilocybin infusion, which remained elevated ($p \leq 0.039$) for the duration of the infusion period. By contrast, the peak frequency in the medium gamma band (Fig. 3F) showed a significant increase within the first 10 min of 10 mg/kg psilocybin infusion. The increase lasted for 40 min of infusion ($p \leq 0.0014$), after which the peak frequency decreased below saline levels ($p \leq 0.0018$). Finally, the high gamma peak frequency (Fig. 3G) showed a transient decrease after 10 min of 1 mg/kg psilocybin infusion ($p = 0.036$), and a sustained decrease after 30 min of 10 mg/kg psilocybin ($p \leq 0.0026$).

In addition to altering the peak oscillating frequency in theta, medium gamma, and high gamma bands, the psilocybin infusion dose-dependently altered the peak amplitude in these bands. Relative to saline infusion, theta peak amplitude (Fig. 3H) decreased after 40 min of 1 mg/kg psilocybin infusion ($p \leq 0.020$) and after only 10 min of 10 mg/kg psilocybin infusion ($p \leq 0.039$). In contrast, the peak amplitude in the medium gamma band (Fig. 3I) showed a significant increase ($p \leq 0.0032$) after 20 min of 1 mg/kg psilocybin infusion and within 10 min of 10 mg/kg psilocybin ($p \leq 0.00050$), both of which remained elevated for the duration of the recording. Similarly, peak amplitude in the high gamma band (Fig. 3J) showed a significant increase ($p \leq 0.044$) after 30 min of 1 mg/kg psilocybin infusion and within 10 min of 10 mg/kg infusion ($p \leq 0.040$), after which high gamma power remained elevated throughout the recording period (Fig. 3J). In summary, spectral analysis of EEG dynamics during continuous psilocybin infusion indicated two distinct EEG states during the 10 mg/kg infusion. The initial period during 10 mg/kg infusion and later period during 1 mg/kg infusion were characterized by decreased theta and increased medium and high gamma power, along with a faster medium gamma peak frequency. As the 10 mg/kg infusion continued, it diverged from the lower dose, characterized by slowing theta and gamma peak frequencies. These data suggest that increasing doses of psilocybin may not have a linear effect on oscillatory brain dynamics.

Psilocybin disrupted theta-gamma coupling in a dose-dependent manner

Theta- and gamma- range oscillations are known to be phase-amplitude coupled, with the phase of theta acting as a timing mechanism for local gamma amplitude [24]. This coupling is believed to support cognitive functions, such as memory and attention, and is altered during changes in states of consciousness [25–27]. Furthermore, recent studies have reported altered timing between spikes and the phase of local field potentials in rodents during lysergic acid diethylamide (LSD) and 2,5-Dimethoxy-4-Iodoamphetamine (DOI) administration [18]. As compared to saline infusion, 0.1 mg/kg psilocybin did not produce any statistically significant changes in either theta-medium gamma or theta-high gamma PAC ($p > 0.05$; Fig. 4). In contrast, both 1 and 10 mg/kg psilocybin infusion diminished theta-medium gamma PAC across the entire cortex (Fig. 4A). After 20 min of 1 mg/kg infusion, there was a decrease in theta-medium gamma PAC in the frontal ($p \leq 0.047$) and posterior/occipital areas ($p \leq 0.049$), which, during the last 20 min of 1 mg/kg infusion, spread to the rest of the cortex ($p \leq 0.045$). The PAC values started to recover back to saline values after the cessation of psilocybin infusion but remained significantly low at the end of 20 min post-infusion period ($p \leq 0.038$). The effect of 10 mg/kg psilocybin on theta-medium gamma PAC (Fig. 4A) was similar, but the onset time was faster (10 min after 10 mg/kg compared to 20 min after 1 mg/kg psilocybin). Interestingly, theta-high gamma PAC (Fig. 4B) was only mildly affected by 1 mg/kg of psilocybin and with late onset (after 40 min of infusion). The decrease was restricted primarily to the frontal regions ($p < 0.05$), which returned to saline values within 10 min after cessation of psilocybin infusion. The 10 mg/kg dose of psilocybin had a much stronger effect on theta-high gamma PAC, which showed widespread decreases across the cortex after 10 min of infusion ($p \leq 0.048$) and which remained significantly low through the post-infusion period (Fig. 4B). In summary, psilocybin infusion dose-dependently disrupted local theta-gamma coupling across

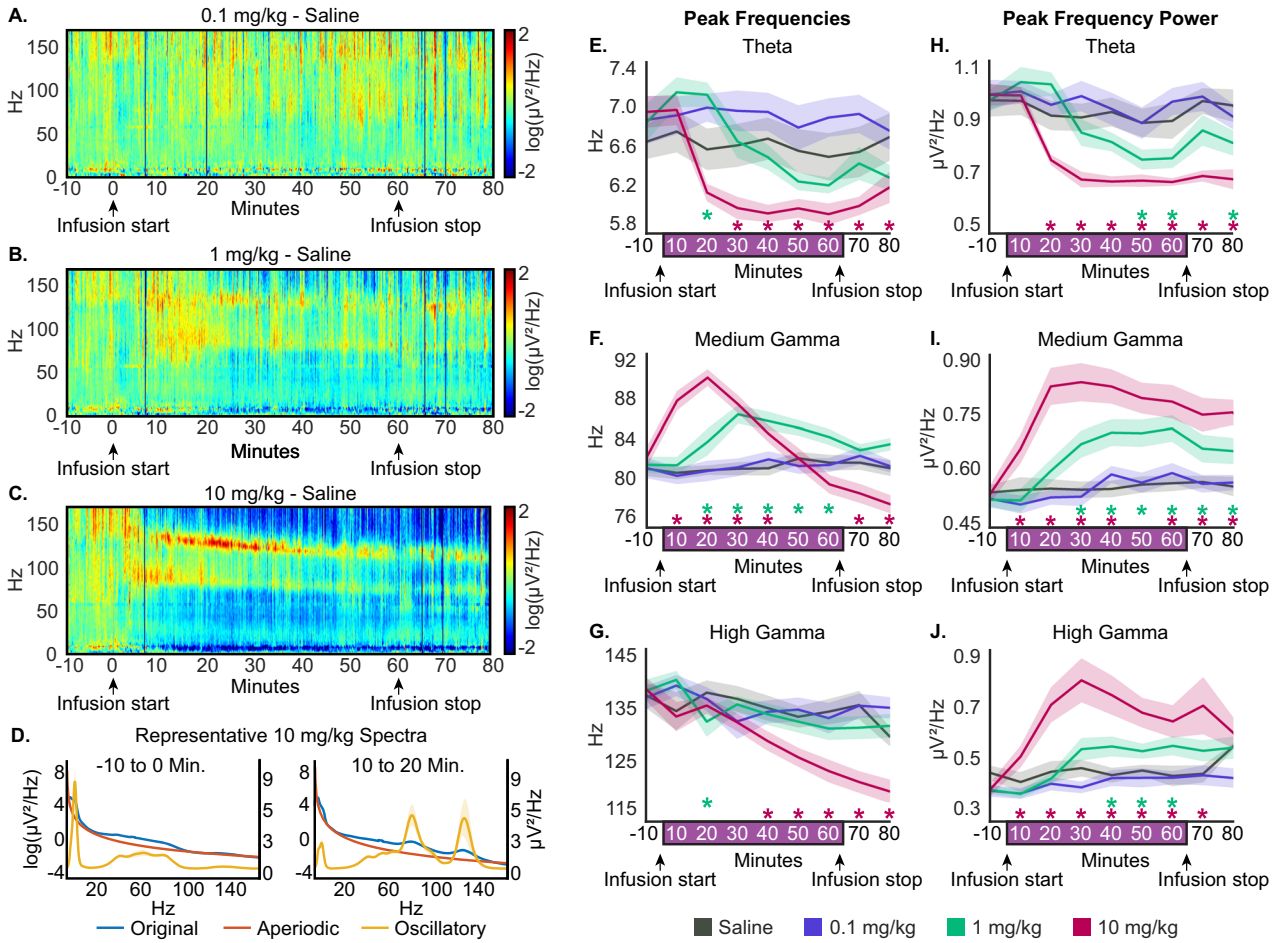

Fig. 3 Intravenous psilocybin altered global peak oscillatory frequencies and amplitudes in a dose-dependent manner. A–C Global spectrograms averaged across rats ($n = 12$, 6 male, 6 female) depicting the difference between each dose (0.1, 1, and 10 mg/kg) and saline. Psilocybin/saline infusion started at time = 0 min and stopped at time = 60 min. Warm colors indicate higher spectral power while cool colors indicate lower spectral power relative to saline. **D** Representative global power spectrum averaged over minutes −10 to 0 (left) and 10–20 (right) of 10 mg/kg psilocybin dose. The FOOOF algorithm was used to model and remove the 1/f component from the original power spectrum to quantify band-specific peak frequencies and amplitudes. Displayed here are the original power spectrum (blue), the aperiodic component (red), and the oscillatory component (gold). For visualization purposes, the original and aperiodic spectra are log-transformed (left y-axis) and the oscillatory spectra are on a linear scale (right y-axis). **E–J** Changes in peak frequency and amplitude in the theta, medium gamma, and high gamma bands. The 1 mg/kg of psilocybin slowed theta peak frequency and increased medium gamma peak frequency. The 10 mg/kg psilocybin dose caused a significant decrease in theta peak frequency. The 10 mg/kg dose initially increased medium gamma peak frequency, but towards the end of infusion the peak frequency slowed relative to saline. The 1 and 10 mg/kg doses of psilocybin decreased theta amplitude and increased medium and high gamma amplitudes relative to saline. The data are provided as mean ± standard error of the mean. *$p < 0.05$, FDR-corrected post-hoc comparisons. The exact p values are provided in the results section.

the cortex, but particularly in frontal cortex, potentially dysregulating corticocortical information coordination.

Psilocybin induced multi-scale reorganization of cortical connectivity in a dose-dependent manner

Functional network reorganization is a key component of current neuronal models of the psychedelic state [17, 38, 39]. Therefore, next, we assessed if the psilocybin-induced dysregulation of local timing between theta and gamma oscillations is accompanied by reorganization of connectivity patterns and network structure in these frequency bands. To characterize psilocybin-induced changes in network organization, we assessed node degree, which is an index of network density or the number of functional connections at a given electrode, and edge-wise wPLI-based connection strength (Fig. 5), before, during, and after psilocybin infusion.

In accordance with the spectral and PAC analyses, there was no effect of 0.1 mg/kg psilocybin infusion on network density or network connectivity strength in any of the frequency bands measured, while both 1 and 10 mg/kg infusions resulted in pronounced multiscale network alterations (Fig. 5). The posterior theta network density (Fig. 5A) was transiently increased after 60 min of 1 mg/kg psilocybin infusion, before returning to saline levels within 20 min post-infusion ($p \leq 0.045$). By contrast, the 10 mg/kg psilocybin infusion rapidly increased theta network density, particularly at posterior electrodes, within 10 min of infusion ($p \leq 0.046$). This effect peaked after 20 min of infusion and returned to saline levels after 40 min of infusion. Paralleling the observed changes in theta network density, frontoparietal theta network connectivity was strengthened ($p \leq 0.047$) only across a few electrodes starting after 30 min infusion of 1 mg/kg psilocybin, whereas the 10 mg/kg psilocybin infusion showed a strong, dynamic effect on theta frontoparietal networks. Theta connection strength increased within 10 min of the 10 mg/kg infusion ($p \leq 0.049$), peaked after 30 min of infusion, then began to decrease, returning to saline levels by 20 min post-infusion.

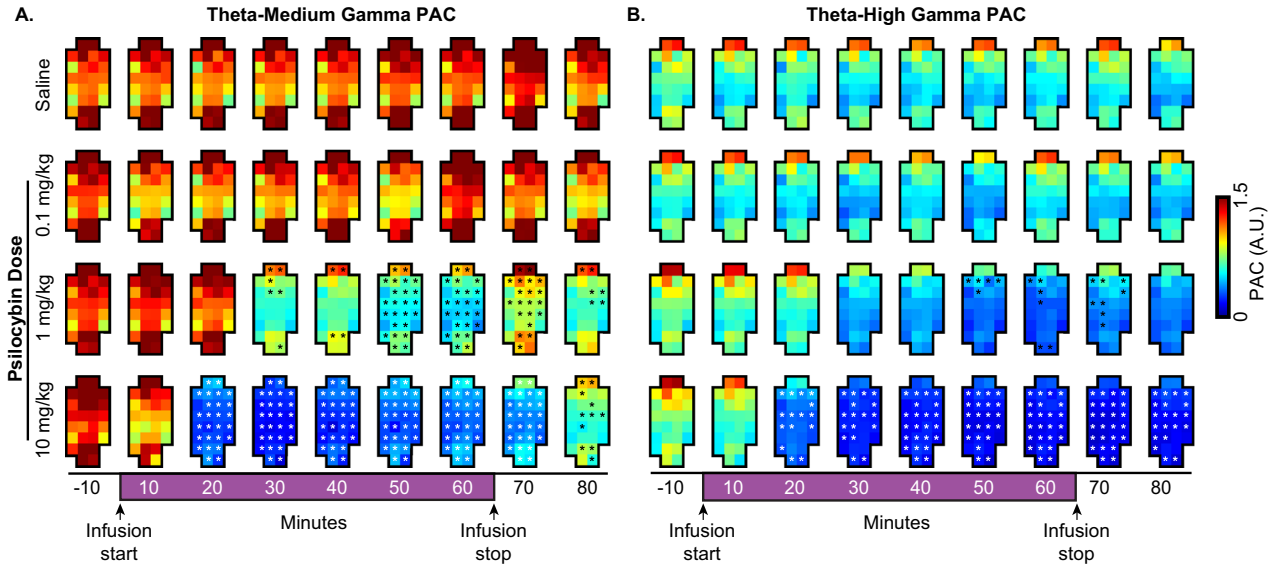

Fig. 4 Intravenous administration of psilocybin dose-dependently disrupted theta-gamma coupling. Following psilocybin infusion, both the 1 and 10 mg/kg doses resulted in decoupling of theta phase from medium **A** and high **B** gamma amplitudes in a dose-dependent fashion. The phase amplitude coupling (PAC) was not altered by the 0.1 mg/kg dose. Each grid represents a 10-min average of PAC values across all rats ($n = 12$, 6 male, 6 female). Each square indicates an electrode in the layout described in Fig. 1. White and black asterisks: *$p < 0.05$, FDR-corrected post-hoc comparisons. The exact p values are provided in the results section.

Unlike the theta network, none of the psilocybin doses altered medium gamma network density relative to saline ($p > 0.05$; Fig. 5B). Although network density was constant, both the 1 and 10 mg/kg doses of psilocybin had a biphasic effect on medium gamma frontoparietal network strength. Medium gamma frontal network synchronization was initially strengthened beginning after 20 and within 10 min of 1 and 10 mg/kg infusions, respectively ($p < 0.05$). After continued infusion, both the 1 and 10 mg/kg doses of psilocybin induced widespread weakening of posterior-clustered medium gamma network connections beginning after 30 and 10 min of infusion, respectively ($p < 0.05$).

High gamma network density and synchronization showed strong modulation by psilocybin infusion (Fig. 5C). Compared to saline infusion, psilocybin administration caused a widespread increase in network density and synchronization strength, particularly in long-range connections to and from the frontal cortex, reflecting a marked change in brain network organization. Both the 1 mg/kg ($p \leq 0.049$) and 10 mg/kg ($p < 0.05$) doses of psilocybin infusion resulted in increased frontal and posterior node degree beginning after 20 and 10 min of infusion, respectively. Similarly, local- and long-range frontoparietal synchronization was increased by both 1 mg/kg ($p < 0.05$) and 10 mg/kg ($p \leq 0.048$) doses, again in a dose-dependent manner, beginning after 20 min and within 10 min of infusion, respectively.

In summary, psilocybin strengthened and broadened the frontal high gamma network in a dose-dependent manner, whereas psilocybin dose had a nonlinear effect on both posterior theta network density and connection strength, as well as medium gamma frontoparietal connectivity, suggesting two distinct states for lower and higher doses of psilocybin. These reorganized connectivity patterns may be enabled by psilocybin-associated loss of local PAC-based modulation of theta and gamma band temporal dynamics.

DISCUSSION

Large-scale network reorganization is consistently reported in human psychedelic studies [8, 10, 11, 17, 40], and although the particular dynamics reported can vary considerably, reconfigured cortical network dynamics are believed to play a role in enabling the psychedelic-associated altered state of consciousness. In this study, we report that intravenous psilocybin infusion has a nonlinear effect on brain network dynamics, resulting in two distinct brain network configurations that emerged over the course of infusion. The 1 mg/kg infusion and the first half of the 10 mg/kg infusion period were primarily characterized by a high-density posterior theta and frontal high gamma network, with strengthened frontoparietal medium gamma connectivity, and cortex-wide decoupling of theta phase from gamma amplitudes. During the later portion of the 10 mg/kg infusion, the brain network state became dominated by the frontal high gamma network as the posterior theta density decreased and frontoparietal medium gamma connectivity continued to weaken. The use of the continuous infusion method ensured that the plasma/brain levels of psilocybin, and therefore the levels of psilocin, which is psilocybin's active metabolite, increased continuously rather than as a step function as would be expected after a bolus administration. Based on the temporal emergence of changes in EEG, it can be inferred that the lower dose of psilocybin (based on cumulative dose administered) activates the posterior theta network by increasing the node degree and connection strength, which is diminished and is accompanied by the activation of frontal gamma network at higher psilocybin concentrations.

To our knowledge, this is the first study to report network dynamics during psilocybin administration in rodents. Continuous infusion, as opposed to a bolus, allowed us to observe the gradual appearance of changes in behavior and EEG. Given the lack of a verbal report of experience, the changes in EEG are most informative, which appeared within the first 10 min of infusion of high dose psilocybin and are consistent with quick onset of the effect of serotonergic psychedelics in human subjects [41, 42]. In a recent study, Vejmola and colleagues [21] reported cortex-wide decrease in spectral power below 40 Hz and localized decreases in corticocortical coherence below 14 Hz after subcutaneous psilocin – the active metabolite of psilocybin – administration in rats. Another recent study by Thomas and colleagues [23] reported that intraperitoneal psilocin administration affects both global vigilance state control and local sleep homeostasis, and acute EEG responses were associated with enhanced 4 Hz oscillatory activity. However, the use of a sparse electrode array with limited spatial

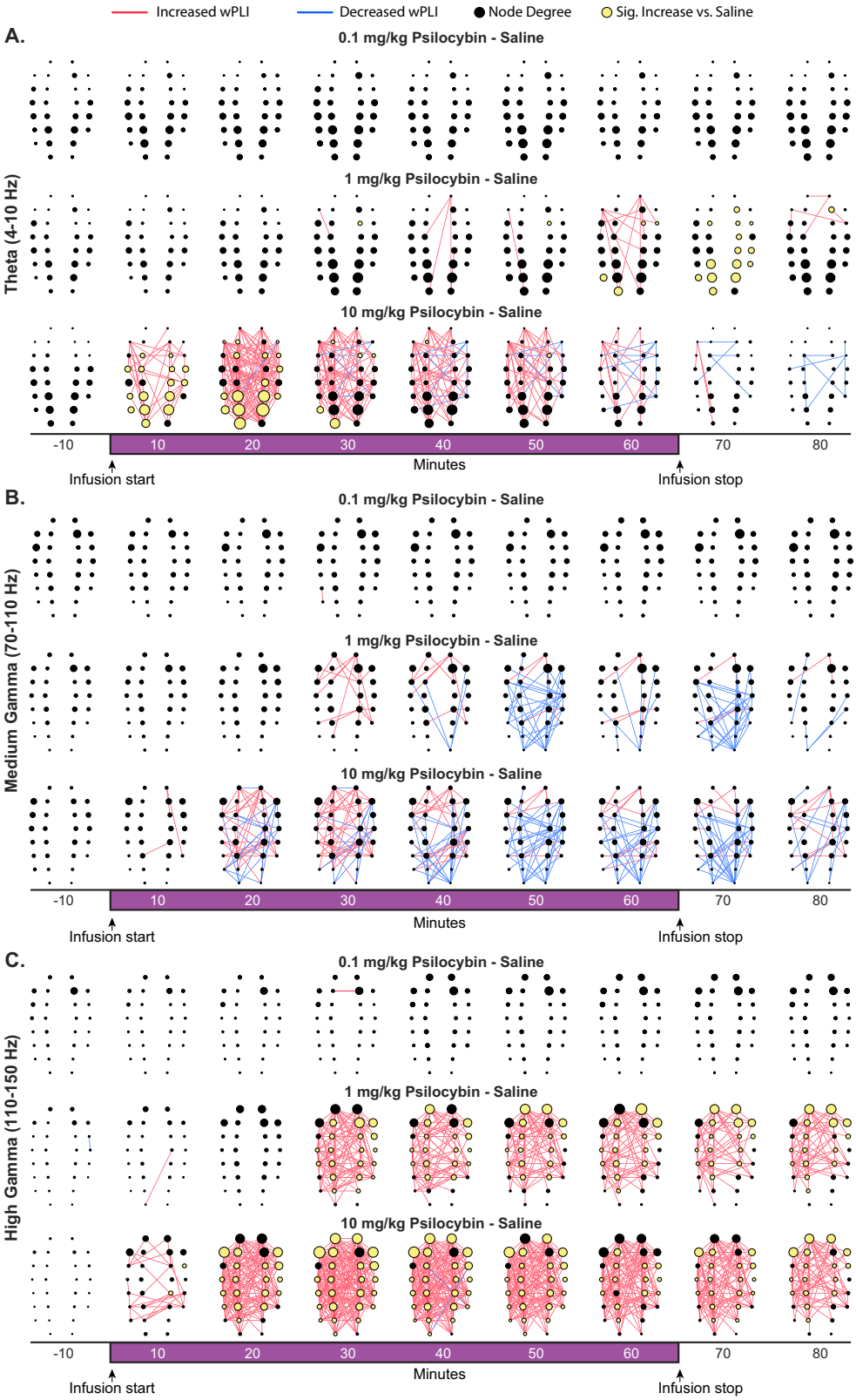

resolution precluded any form of EEG network analysis, and the EEG findings were limited to low frequency (<40 Hz) oscillations [21, 23]. Of note, the divergence in theta band connectivity findings between our study and Vejmola et al. [21] is likely due to methodological differences. Instead of coherence, our study utilized wPLI, which is robust to volume conduction and therefore may differ from coherence especially in low-frequency, high-amplitude bands such as theta. Differences in brain dynamics between all three studies could also be due to the different routes of administration.

Fig. 5 Intravenous administration of psilocybin induced broad reorganization of theta and gamma cortical connectivity patterns. wPLI connectivity differences between psilocybin and saline averaged across rats ($n = 12$, 6 male, 6 female) and over 10-min bins. Red lines indicate increased wPLI relative to saline, blue lines indicate decreased wPLI relative to saline. Black dots indicate electrode location corresponding to the electrode map shown in Fig. 1. Dot size indicates the magnitude of node degree. Yellow dots show significantly increased node degree relative to saline. Only connections that were significantly different ($p < 0.05$) from saline following FDR-correction are displayed. Beginning halfway through infusion, the 1 mg/kg psilocybin dose caused sparse increases in frontoparietal theta connectivity **A**, increased medium gamma frontal connectivity, but decreased posterior connectivity **B**, and caused broad frontoparietal increases in high gamma connectivity **C**. The 10 mg/kg psilocybin dose had a similar effect on cortical connectivity, but was amplified in a dose-dependent fashion, in particular causing large increases in theta posterior connectivity **A**, increasing, then decreasing medium gamma frontoparietal connectivity **B**, and increasing frontoparietal high gamma connectivity **C**. The exact p values are provided in the results section.

A notable feature of the network results presented here is the simultaneous change in the theta posterior network and the frontal high gamma network, which partially overlap. Several reports of human fMRI data indicate that psilocybin likely results in a reorganization of functional network topology [8, 17, 43]. The increased frontal high gamma network density, nonlinear changes in posterior theta network density, and broad modulation of frontoposterior connectivity strengths across theta and gamma bands are consistent with human fMRI data indicating increased long-range between-network connectivity [11] as well as reports that, during psilocybin administration, the spatial distribution of long-range networks varies over time [10, 16].

A growing body of literature emphasizes the role of frontoposterior high gamma connectivity during psychedelic administration in rodents and humans [14, 18, 22, 39, 44]. Increased high gamma frontoposterior and frontostriatal connectivity has been reported in rodents administered serotonergic psychedelics such as LSD, DOI, and atypical psychedelics such as ketamine, nitrous oxide, and phencyclidine [18–20, 45]. These long-range networks may play an important role in facilitating a psychedelic state; for example, in humans, increased long-range connectivity is correlated with blood plasma levels of psilocybin and subjective drug-induced experience [11, 12].

Local cortical circuit conditions also play a significant role in determining large-scale network synchronization. Several rodent studies of 5HT2A- and NMDA-associated psychedelics have used depth electrodes to localize high gamma activity to sites in frontal cortex, including olfactory cortex, orbital cortex, medial prefrontal cortex, and anterior cingulate cortex as well as in parietal cortical areas of sensorimotor cortex and subcortical sites in striatum and nucleus accumbens [18, 22, 45]. Similarly, decoupling of local spiking activity from the phase of low frequency local field potentials has also been observed following psilocybin, LSD, DOI, ketamine, and phencyclidine administration in rodents [18, 22], which parallels the dose-dependent loss of theta-gamma coupling observed in our data. Gamma peak frequency may be partially determined by the balance of excitatory and inhibitory activity [46] and has been shown to be an important index of changing cortical conditions associated with both cognitive demand and level of arousal [47]. The increased high gamma network activation and associated increased gamma power may also have relevance for the neuroplastic effects of psilocybin. Recent evidence indicates that psychedelics activate BDNF and mTOR signaling pathways which result in structural changes such as acute and lasting increases in dendritic spine density [48–50]. Synaptic plasticity has also been associated with the increased spiking activity [51] that generates local increases in gamma (>70 Hz) power [52, 53]. However, further research is necessary to directly link psychedelic-induced high gamma activity to changes in neuroplasticity.

There are several caveats to our study. First, the increase in connectivity between association cortices does not rule out significant roles for the claustrum, basal ganglia, thalamus, or cerebellum, which are key to some models of psychedelic action [38, 54]. Second, because wPLI does not provide direction of influence, our data do not provide evidence for a "top down" or "bottom up" mechanism for the psilocybin state. Third, although 5-HT2A receptors are widely accepted to mediate the psychedelic effects after psilocybin administration, our study lacks the causal data to demonstrate this relationship. Fourth, it is important to note that due to the lack of verbal report or an objective measure to report 'content' of consciousness in animals, we cannot comment on the presence or absence of psychedelic experience. Lastly, although it is difficult to separate the drug effects from the state effects, at least without verbal report and extensive mechanistic testing, our results suggest that psilocybin induced a combination of both drug and state effects. The drug effect is illustrated by the disappearance of EEG changes after cessation of psilocybin administration, and the state effect is evident in the changes in EEG dynamics during psilocybin-induced decrease in motor activity.

Overall, our results demonstrate that psilocybin produced nonlinear multiscale changes in network organization, which are consistent with fMRI reports of shifting patterns of decreased within-network and increased between-network connectivity [11, 15, 43]. The two distinct phases of theta network density and medium gamma network strength, suggest that rather than having a linear effect on brain network dynamics, higher doses of psilocybin likely produce a brain state distinct from lower doses. Of note, the changes in EEG gamma connectivity occurred in the absence of any behavioral activity or after the psilocybin induced locomotion and/or HTR ceased. This dissociation prompts further careful investigation of HTR as a surrogate for the non-ordinary state induced by psychedelic drugs in rodents.

DATA AVAILABILITY

The raw data can be made available upon request to the corresponding author, DP, dineshp@umich.edu.

CODE AVAILABILITY

The code utilized in this article can be made available upon request to the corresponding author, DP, dineshp@umich.edu.

REFERENCES

1. Gukasyan N, Davis AK, Barrett FS, Cosimano MP, Sepeda ND, Johnson MW, et al. Efficacy and safety of psilocybin-assisted treatment for major depressive disorder: prospective 12-month follow-up. J Psychopharmacol. 2022;36:151–8.
2. Griffiths RR, Johnson MW, Carducci MA, Umbricht A, Richards WA, Richards BD, et al. Psilocybin produces substantial and sustained decreases in depression and anxiety in patients with life-threatening cancer: a randomized double-blind trial. J Psychopharmacol. 2016;30:1181–97.
3. Davis AK, Barrett FS, May DG, Cosimano MP, Sepeda ND, Johnson MW, et al. Effects of psilocybin-assisted therapy on major depressive disorder: a randomized clinical trial. JAMA Psychiatry. 2021;78:1.
4. Raison CL, Sanacora G, Woolley J, Heinzerling K, Dunlop BW, Brown RT, et al. Single-dose psilocybin treatment for major depressive disorder: a randomized clinical trial. JAMA. 2023;330:843–53.
5. Bogenschutz MP, Ross S, Bhatt S, Baron T, Forcehimes AA, Laska E, et al. Percentage of heavy drinking days following psilocybin-assisted psychotherapy vs placebo in the treatment of adult patients with alcohol use disorder: a randomized clinical trial. JAMA Psychiatry. 2022;79:953.

6. von Rotz R, Schindowski EM, Jungwirth J, Schuldt A, Rieser NM, Zahoranszky K, et al. Single-dose psilocybin-assisted therapy in major depressive disorder: a placebo-controlled, double-blind, randomised clinical trial. EClinicalMedicine. 2023;56:101809.
7. Preller KH, Duerler P, Burt JB, Ji JL, Adkinson B, Stämpfli P, et al. Psilocybin induces time-dependent changes in global functional connectivity. Biol Psychiatry. 2020;88:197–207.
8. Tagliazucchi E, Carhart-Harris R, Leech R, Nutt D, Chialvo DR. Enhanced repertoire of brain dynamical states during the psychedelic experience. Hum Brain Mapp. 2014;35:5442–56.
9. Schartner MM, Carhart-Harris RL, Barrett AB, Seth AK, Muthukumaraswamy SD. Increased spontaneous MEG signal diversity for psychoactive doses of ketamine, LSD and psilocybin. Sci Rep. 2017;7:1–12.
10. Lord LD, Expert P, Atasoy S, Roseman L, Rapuano K, Lambiotte R, et al. Dynamical exploration of the repertoire of brain networks at rest is modulated by psilocybin. Neuroimage. 2019;199:127–42.
11. Madsen MK, Stenbæk DS, Arvidsson A, Armand S, Marstrand-Joergensen MR, Johansen SS, et al. Psilocybin-induced changes in brain network integrity and segregation correlate with plasma psilocin level and psychedelic experience. Eur Neuropsychopharmacol. 2021;50:121–32.
12. Kometer M, Pokorny T, Seifritz E, Volleinweider FX. Psilocybin-induced spiritual experiences and insightfulness are associated with synchronization of neuronal oscillations. Psychopharmacology (Berl). 2015;232:3663–76.
13. Pallavicini C, Vilas MG, Villarreal M, Zamberlan F, Muthukumaraswamy S, Nutt D, et al. Spectral signatures of serotonergic psychedelics and glutamatergic dissociatives. Neuroimage. 2019;200:281–91.
14. Muthukumaraswamy SD, Carhart-Harris RL, Moran RJ, Brookes MJ, Williams TM, Errtizoe D, et al. Broadband cortical desynchronization underlies the human psychedelic state. J Neurosci. 2013;33:15171–83.
15. Lebedev AV, Lövdén M, Rosenthal G, Feilding A, Nutt DJ, Carhart-Harris RL. Finding the self by losing the self: neural correlates of ego-dissolution under psilocybin. Hum Brain Mapp. 2015;36:3137–53. https://doi.org/10.1002/hbm.22833
16. Olsen AS, Lykkebo-Valløe A, Ozenne B, Madsen MK, Stenbæk DS, Armand S, et al. Psilocybin modulation of time-varying functional connectivity is associated with plasma psilocin and subjective effects. Neuroimage. 2022;264:119716.
17. Siegel JS, Subramanian S, Perry D, Kay BP, Gordon EM, Laumann TO, et al. Psilocybin desynchronizes the human brain. Nature. 2024;632:131–8.
18. Brys I, Barrientos SA, Ward JE, Wallander J, Petersson P, Halje P. 5-HT2AR and NMDAR psychedelics induce similar hyper-synchronous states in the rat cognitive-limbic cortex-basal ganglia system. Commun Biol. 2023;6:1–13.
19. Brito MA, Li D, Fields CW, Rybicki-Kler C, Dean JG, Liu T, et al. Cortical acetylcholine levels correlate with neurophysiologic complexity during subanesthetic ketamine and nitrous oxide exposure in rats. Anesth Analg. 2022;134:1126.
20. Pal D, Hambrecht-Wiedbusch VS, Silverstein BH, Mashour GA. Electroencephalographic coherence and cortical acetylcholine during ketamine-induced unconsciousness. Br J Anaesth. 2015;114:979–89.
21. Vejmola Č, Tylš F, Piorecká V, Koudelka V, Kadeřábek L, Novák T, et al. Psilocin, LSD, mescaline, and DOB all induce broadband desynchronization of EEG and disconnection in rats with robust translational validity. Transl Psychiatry. 2021;11:1–8.
22. Golden CT, Chadderton P. Psilocybin reduces low frequency oscillatory power and neuronal phase-locking in the anterior cingulate cortex of awake rodents. Sci Rep. 2022;12:1–12.
23. Thomas CW, Blanco-Duque C, Bréant BJ, Goodwin GM, Sharp T, Bannerman DM, et al. Psilocin acutely alters sleep-wake architecture and cortical brain activity in laboratory mice. Transl Psychiatry. 2022;12:1–13.
24. Bonnefond M, Kastner S, Jensen O. Communication between brain areas based on nested oscillations. eNeuro. 2017;4:ENEURO.0153-16.2017.
25. Pal D, Silverstein BH, Sharba L, Li D, Hambrecht-Wiedbusch VS, Hudetz AG, et al. Propofol, sevoflurane, and ketamine induce a reversible increase in delta-gamma and theta-gamma phase-amplitude coupling in frontal cortex of rat. Front Syst Neurosci. 2017;11:41.
26. Voytek B, Kayser AS, Badre D, Fegen D, Chang EF, Crone NE, et al. Oscillatory dynamics coordinating human frontal networks in support of goal maintenance. Nat Neurosci. 2015;18:1318–24.
27. Helfrich RF, Knight RT. Oscillatory dynamics of prefrontal cognitive control. Trends Cogn Sci. 2016;20:916–30.
28. Kilkenny C, Browne W, Cuthill IC, Emerson M, Altman DG. Animal research: reporting in vivo experiments: the ARRIVE guidelines. J Gene Med. 2010;12:561–3.
29. Halberstadt AL, Koedood L, Powell SB, Geyer MA. Differential contributions of serotonin receptors to the behavioral effects of indoleamine hallucinogens in mice. J Psychopharmacol. 2011;25:1548–61.
30. Halberstadt AL, Geyer MA. Multiple receptors contribute to the behavioral effects of indoleamine hallucinogens. Neuropharmacology. 2011;61:364–81.
31. Canal CE, Morgan D. Head-twitch response in rodents induced by the hallucinogen 2,5-dimethoxy-4-iodoamphetamine: a comprehensive history, a re-evaluation of mechanisms, and its utility as a model. Drug Test Anal. 2012;4:556–76.
32. Oostenveld R, Fries P, Maris E, Schoffelen JM. FieldTrip: open source software for advanced analysis of MEG, EEG, and invasive electrophysiological data. Comput Intell Neurosci. 2011;2011:156869. https://doi.org/10.1155/2011/156869
33. Donoghue T, Haller M, Peterson EJ, Varma P, Sebastian P, Gao R, et al. Parameterizing neural power spectra into periodic and aperiodic components. Nat Neurosci. 2020;23:1655–65.
34. Canolty RT, Edwards E, Dalal SS, Soltani M, Nagarajan SS, Kirsch HE, et al. High gamma power is phase-locked to theta oscillations in human neocortex. Science. 2006;313:1626–8.
35. Onslow ACE, Bogacz R, Jones MW. Quantifying phase-amplitude coupling in neuronal network oscillations. Prog Biophys Mol Biol. 2011;105:49–57.
36. Vinck M, Oostenveld R, Van Wingerden M, Battaglia F, Pennartz CMA. An improved index of phase-synchronization for electrophysiological data in the presence of volume-conduction, noise and sample-size bias. Neuroimage. 2011;55:1548–65.
37. Theiler J, Galdrikian B, Longtin A, Eubank S, Farmer JD. Testing for nonlinearity in time series the method of surrogate data. Washington, D.C.: Oak Ridge, Tenn.: United States. Dept. of Defense; distributed by the Office of Scientific and Technical Information, U.S. Dept. of Energy; 1991. http://www.osti.gov/servlets/purl/6026813/
38. Doss MK, Madden MB, Gaddis A, Nebel MB, Griffiths RR, Mathur BN, et al. Models of psychedelic drug action: modulation of cortical-subcortical circuits. Brain. 2022;145:441–56.
39. Carhart-Harris RL, Friston KJ. REBUS and the anarchic brain: toward a unified model of the brain action of psychedelics. Pharmacol Rev. 2019;71:316–44.
40. Müller F, Dolder PC, Schmidt A, Liechti ME, Borgwardt S. Altered network hub connectivity after acute LSD administration. Neuroimage Clin. 2018;18:694.
41. Carhart-Harris RL, Williams TM, Sessa B, Tyacke RJ, Rich AS, Feilding A, et al. The administration of psilocybin to healthy, hallucinogen-experienced volunteers in a mock-functional magnetic resonance imaging environment: a preliminary investigation of tolerability. J Psychopharmacol. 2011;25:1562–7.
42. Carhart-Harris RL, Erritzoe D, Williams T, Stone JM, Reed LJ, Colasanti A, et al. Neural correlates of the psychedelic state as determined by fMRI studies with psilocybin. Proc Natl Acad Sci USA. 2012;109:2138–43.
43. McCulloch DEW, Knudsen GM, Barrett FS, Doss MK, Carhart-Harris RL, Rosas FE, et al. Psychedelic resting-state neuroimaging: a review and perspective on balancing replication and novel analyses. Neurosci Biobehav Rev. 2022;138:104689.
44. Mason NL, Kuypers KPC, Müller F, Reckweg J, Tse DHY, Toennes SW, et al. Me, myself, bye: regional alterations in glutamate and the experience of ego dissolution with psilocybin. Neuropsychopharmacology. 2020;45:2003.
45. Goda SA, Piasecka J, Olszewski M, Kasicki S, Hunt MJ. Serotonergic hallucinogens differentially modify gamma and high frequency oscillations in the rat nucleus accumbens. Psychopharmacology (Berl). 2013;228:271.
46. Atallah BV, Scanziani M. Instantaneous modulation of gamma oscillation frequency by balancing excitation with inhibition. Neuron. 2009;62:566–77.
47. Mockevičius A, Šveistytė K, Griškova-Bulanova I. Individual/Peak gamma frequency: what do we know? Brain Sci. 2023;13:792.
48. Ly C, Greb AC, Cameron LP, Wong JM, Barragan EV, Wilson PC, et al. Psychedelics promote structural and functional neural plasticity. Cell Rep. 2018;23:3170.
49. Shao LX, Liao C, Gregg I, Davoudian PA, Savalia NK, Delagarza K, et al. Psilocybin induces rapid and persistent growth of dendritic spines in frontal cortex in vivo. Neuron. 2021;109:2535.
50. Husain MI, Ledwos N, Fellows E, Baer J, Rosenblat JD, Blumberger DM, et al. Serotonergic psychedelics for depression: what do we know about neurobiological mechanisms of action? Front Psychiatry. 2023;13:1076459.
51. Wang M, Liao X, Li R, Liang S, Ding R, Li J, et al. Single-neuron representation of learned complex sounds in the auditory cortex. Nat Commun. 2020;11:1–14.
52. Buzsáki G, Wang X-J. Mechanisms of gamma oscillations. Annu Rev Neurosci. 2012;35:203–25.
53. Whittingstall K, Logothetis NK. Frequency-band coupling in surface EEG reflects spiking activity in monkey visual cortex. Neuron. 2009;64:281–9.
54. Vollenweider FX, Geyer MA. A systems model of altered consciousness: integrating natural and drug-induced psychoses. Brain Res Bull. 2001;56:495–507.

ACKNOWLEDGEMENTS

We thank Dr. Chris Andrews (Consulting for Statistics, Computing & Analytics Research, University of Michigan, Ann Arbor, Michigan) for consultation and help with the statistical analysis. The research reported in this study was supported by the National Institutes of Health Grants R01GM111293 to GAM and DP, R01GM121919 to DP, funding from Tryp Therapeutics, (Kelowna, British Columbia, V1Y 7T2, Canada) to GV and DP, and the Department of Anesthesiology, University of Michigan Medical School, Ann Arbor, MI.

AUTHOR CONTRIBUTIONS

BHS, NK, GV, DP, designed the research; NK and TL performed the experiments; all authors contributed to drafting the article; BHS, NK, AN, UL, GAM, GV, DP, interpreted the data and wrote the article.

COMPETING INTERESTS

Jim Gilligan, Ph.D. is President & Chief Scientific Officer at Tryp Therapeutics. Peter Guzzo, PhD is Consulting VP, Drug Development at Tryp Therapeutics.

ETHICS APPROVAL AND CONSENT TO PARTICIPATE

All experiments were approved by the Institutional Animal Care and Use Committee at the University of Michigan, Ann Arbor, and were conducted in compliance with the Guide for the Care and Use of Laboratory Animals (Ed 8, National Academies Press) and ARRIVE Guidelines.

ADDITIONAL INFORMATION

Supplementary information The online version contains supplementary material available at https://doi.org/10.1038/s41398-025-03308-4.

Correspondence and requests for materials should be addressed to Dinesh Pal.